INL/CON-05-00304
PREPRINT

Electrolytic Reduction of Spent Oxide Fuel -- Bench-Scale Test Results

Global 2005

Steven D. Herrmann
Shelly X. Li
Michael F. Simpson

October 2005

The INL is a
U.S. Department of Energy
National Laboratory
operated by
Battelle Energy Alliance

Proceedings of GLOBAL 2005
Tsukuba, Japan, Oct 9-13, 2005
Paper No. 488

Electrolytic Reduction of Spent Oxide Fuel – Bench-Scale Test Results

Steven D. HERRMANN[1], Shelly X. LI[1], and Michael F. SIMPSON[1]

[1]*Idaho National Laboratory, P.O. Box 1625, Idaho Falls, ID 83415-6180, USA*

Tel. 001-208-533-7859, Fax. 001-208-533-7471, E-mail: steven.herrmann@inl.gov

ABSTRACT: A series of tests were performed to demonstrate the electrolytic reduction of spent light water reactor fuel at bench-scale in a hot cell at the Idaho National Laboratory Materials and Fuels Complex (formerly Argonne National Laboratory – West). The process involves the conversion of oxide fuel to metal by electrolytic means, which would then enable subsequent separation and recovery of actinides via existing electrometallurgical technologies, i.e., electrorefining. Four electrolytic reduction runs were performed at bench scale using ~500 ml of molten LiCl – 1 wt% Li_2O electrolyte at 650 ºC. In each run, ~50 g of crushed spent oxide fuel was loaded into a permeable stainless steel basket and immersed into the electrolyte as the cathode. A spiral wound platinum wire was immersed into the electrolyte as the anode. When a controlled electric current was conducted through the anode and cathode, the oxide fuel was reduced to metal in the basket and oxygen gas was evolved at the anode. Salt samples were extracted before and after each electrolytic reduction run and analyzed for fuel and fission product constituents. The fuel baskets following each run were sectioned and sampled, revealing an extent of uranium oxide reduction in excess of 98%.

KEYWORDS: *electrolytic reduction, oxide reduction, pyrochemical processing, electrometallurgical treatment, spent oxide fuel treatment, light water reactor fuel treatment, nuclear fuel reprocessing, nuclear fuel recycle.*

I. INTRODUCTION

The electrometallurgical treatment of irradiated metal fuel from Experimental Breeder Reactor II (EBR-II) has been ongoing since 1996 at the Idaho National Laboratory Materials and Fuels Complex (formerly Argonne National Laboratory – West). The electrometallurgical treatment of metal fuel involves the anodic dissolution of the fuel in a molten LiCl/KCl/UCl_3 electrolyte and the simultaneous cathodic deposition and recovery of refined fuel (separated from fission products and cladding) in an electrorefiner and associated cathode processing equipment. [1]

In order to extend the electrometallurgical treatment technology to oxide fuels, a head-end process is necessary to convert (reduce) an oxide fuel to metal. Development of such a reduction process has been pursued by Argonne National Laboratory (ANL) and the Idaho National Laboratory (INL). Specifically, the development of an electrolytic reduction process with *unirradiated* fuels has been largely pursued by ANL. [2] A demonstration of the electrolytic reduction process with *spent* fuel was performed at the INL Materials and Fuels Complex, which is the subject of this paper.

In the electrolytic reduction process, oxide fuel is crushed and loaded into a permeable stainless steel basket. The basket is immersed into a molten LiCl – 1 wt% Li_2O electrolyte at 650 ºC and configured to a power supply as the cathode. A platinum wire is likewise immersed into the electrolyte and configured as the anode. An electric current is conducted through the anode and cathode such that the oxide fuel is reduced to metal and retained in the basket. The oxygen ions liberated by the reduction of oxide fuel to metal at the cathode diffuse into the electrolyte and are oxidized to oxygen gas at the platinum anode. Thus, the overall reaction is $M_xO_y \rightarrow xM + y/2\ O_2$ (g), where M = fuel constituent metal. Additional description of the electrolytic reduction process has been documented elsewhere. [3]

A series of electrolytic reduction tests were performed with spent light water reactor fuel in the INL Hot Fuel Examination Facility (HFEF) to demonstrate the reduction process utilizing existing bench-scale electrochemical equipment. The specific objectives of the demonstration were to (1) determine the extent of reduction of metal oxides from the process, (2) examine the distribution of fuel constituents between the liquid (salt) and solid (fuel) phases, and (3) assess the effect that accumulated fission products may have on the process. The following describes the operating conditions, performance, and results of the prescribed tests.

II. OPERATING CONDITIONS

The standard potentials (E^o) for the major constituent reactions in the electrolytic reduction process at 650 ºC are shown below. [4]

$UO_2 \rightarrow U + O_2$	$E^o = 2.40$ V
$Li_2O \rightarrow 2\ Li + ½\ O_2$	$E^o = 2.47$ V
$LiCl \rightarrow Li + ½\ Cl_2$	$E^o = 3.46$ V

The standard potentials of uranium oxide and lithium oxide differ by approximately 70 mV. Even though the prescribed salt system (LiCl – 1 wt% Li_2O) is not at standard conditions,

the potential difference between UO_2 and Li_2O is sufficiently small to make operation of the cell for UO_2 reduction alone difficult. Consequently, the electrolytic reduction tests with spent oxide fuel were conducted such that both uranium and lithium reduction occurred at the cathode. An advantage in lithium metal generation at the location of uranium oxide is it will chemically reduce the oxide fuel as shown below. [4]

$$4\ Li + UO_2 \rightarrow U + 2\ Li_2O \quad \Delta G\ (650^oC) = -27\ kJ/mol$$

A disadvantage in lithium metal generation is its capability of diffusing through the salt and attacking the platinum anode. To mitigate the attack of lithium on the platinum anode, the electrolytic reduction cell was configured with an additional power supply as shown in Figure 1. The current from the primary power supply was controlled to effect the reduction of uranium oxide and lithium oxide while preventing the anodic dissolution of platinum. The current from the secondary power supply was controlled to mitigate the diffusion of lithium metal outside the cathode basket by oxidizing the lithium metal (to Li^+) upon contact with the basket wall. Thus, the major half-cell and net reactions that occur in this system are listed below.

Primary Power Supply:

Cathode: $UO_2 + 4e^- \rightarrow U + 2\ O^{2-}$
Anode: $2\ O^{2-} \rightarrow O_2\,(g) + 4\ e^-$
Net Reaction: $UO_2 \rightarrow U + O_2\,(g)$

Cathode: $4\ Li^+ + 4e^- \rightarrow 4\ Li$
Anode: $2\ O^{2-} \rightarrow O_2\,(g) + 4\ e^-$
Net Reaction: $4\ Li^+ + 2\ O^{2-} \rightarrow 4\ Li + O_2\,(g)$

Secondary Power Supply:

Cathode: $Li^+ + e^- \rightarrow Li$
Anode: $Li \rightarrow Li^+ + e^-$
Net Reaction: Li/Li^+ cycle

The electrolytic reduction cell was configured with a Ni/NiO reference electrode for monitoring relative anode and cathode potentials. The potential values used in this paper are relative to the Ni/NiO reference electrode, unless otherwise stated.

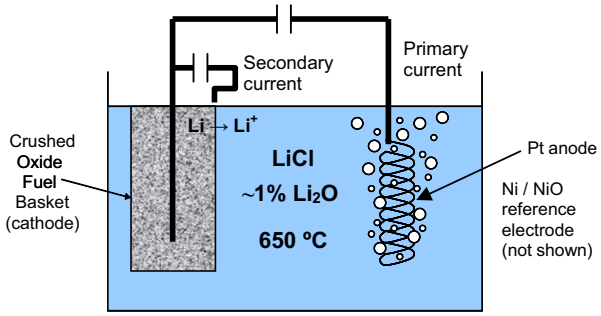

Figure 1. Schematic of Electrolytic Reduction Cell

1. Equipment

The electrolytic reduction tests were performed in an existing electrochemical cell called the Hot Fuel Dissolution Apparatus (HFDA), which is located in an argon atmosphere hot cell (HFEF) at the INL Materials and Fuels Complex. The HFDA consists of a furnace assembly enveloping a 10-cm diameter steel crucible with a set of heat shields that is ported for 5 salt contacting probes – one center port and 4 outer ports that are 90 degrees apart on a 3.5-cm radius. Probes specific to electrolytic reduction operations were fabricated and configured in the HFDA as shown in Figure 2. The steel crucible was lined on the inside with a 10-cm diameter by 11-cm tall magnesia crucible. The fuel baskets were fabricated from a bonded combination of stainless steel perforated sheet metal, 325 mesh wire cloth, and 18 mesh wire cloth to form a 1.9-cm diameter by 5.7-cm tall closed-end cylinder. The top open end of the cylinder was welded to an armature that suspended an electrically isolated stainless steel center lead. The fuel basket was fitted to electrically isolated extension rods, which were connected to the respective power supplies outside the HFDA containment. The anode was located in a port adjacent to the cathode. The anode was fabricated from 1-mm diameter platinum wire that was wound to form a 6-mm diameter by 5-cm tall spiral. Approximately 50 cm of platinum wire was in contact with the salt. A reference electrode was located in the rear port. The reference electrode was fabricated from magnesia tube and configured for a Ni/NiO coupling with the salt. The center port was configured with a thermocouple and the unoccupied port was used for periodic salt sampling.

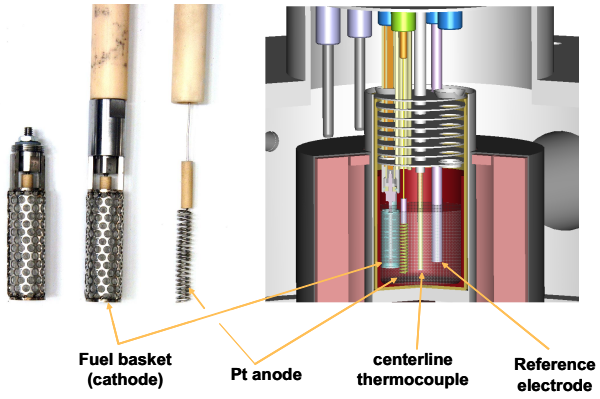

Figure 2. Sectional View of HFDA Cell Configuration for Electrolytic Reduction Operations

The power supplies, potentiometers, and data acquisition systems were located outside the hot cell. Cyclic voltammetry was performed with an EG&G Princeton Applied Research Model 273A Poteniostat/Galvanostat. Data were monitored and recorded with a Hewlett Packard Model 34970A Data Acquisition/Switch Unit. The primary and secondary currents were supplied by KEPCO Bipolar Operational Power Supplies/Amplifiers.

2. Spent Oxide Fuel

The electrolytic reduction tests were conducted with spent

light water reactor fuel from Belgium Reactor 3 (BR3). A number of BR3 fuel elements came to the INL Materials and Fuels Complex for examination and testing in the mid-1980s, and several intact elements remained in storage at the INL. One of these elements was selected for demonstration of the electrolytic reduction process. The characteristics of the BR3 fuel are typical of those for a spent light water reactor fuel with an average burn-up of 4.5 at% and a decay of 25 years. The BR3 fuel element contained an 8-mm by 1000-mm fuel column of UO_2 pellets that were initially enriched to 8.3 wt% in U-235.

The fuel from a single BR3 spent fuel element was removed by cutting the element into nominal 20-cm lengths. The fuel was then crushed and removed from its Zircaloy-4 cladding by use of a slide hammer. The fuel was further crushed and sieved into four particle size ranges of 2.8 mm to 4 mm (87.87 g), 1.2 mm to 2.8 mm (137.79 g), 0.6 to 1.2 mm (105.29 g), and 45 µm to 0.6 mm (99.95 g). A considerable amount of fuel fines of < 45 µm (41.09 g) resulted from the crushing and sieving of the BR3 fuel element. A portion of these fines was removed and submitted for chemical and radiochemical analyses. The analyses revealed constituent concentrations in the BR3 fuel, as categorized in Table I.

Table I. Constituent Concentrations in Spent BR3 Fuel

RE (ppm)		U/TRU (ppm)		NM (ppm)		FPS (ppm)	
Nd	4200	U	838000	Zr	3300	Cs	2500
Ce	2600	Pu	6060	Mo	2600	Ba	2200
La	1300	Np-237	421	Ru	1200	Sr	790
Pr	1200	Am-241	230	Tc	540	Rb	530
Sm	830			Pd	470	Te	490
Y	560			Rh	280	Eu	100
Gd	60			Cd	70		
Dy	10			Ag	45		

Where: RE = rare earth; U = uranium; TRU = transuranic; NM = noble metal; FPS = salt-soluble fission products

III. TEST PERFORMANCE AND RESULTS

Four electrolytic reduction runs with spent BR3 fuel were conducted in the HFDA, as outlined below.

Run No.	1	2	3	4
Fuel Mass	46.71 g	46.01 g	41.0 g	50.3 g
Particle Size	1.2 – 2.8 mm			.045 – 0.6 mm

The first 3 runs were performed successively in the same electrolyte solution, thus allowing salt-soluble fission products to accumulate in the electrolyte. The electrolyte solution was replaced with clean salt for the fourth electrolytic reduction run. After the first electrolyte solution was prepared and before the first BR3 fuel basket was reduced, a series of cyclic voltammetry runs were performed to characterize the electrochemical cell. The electrolytic reduction runs were then performed successively, after which the fuel baskets were sectioned, sampled, and subjected to chemical and radiochemical analyses. The following describes the results of these operations.

1. Cyclic Voltammetry

The first solution of molten salt was prepared by loading 700 g of LiCl (99.99%, <100 ppm moisture) into a magnesia crucible and heating it in the HFDA to 650 ºC. A total of 7 g of Li_2O (99.6%) was added to the LiCl in 4 equal increments. Cyclic voltammetry (CV) runs were performed before and after each Li_2O addition. The CV runs utilized separate stainless steel and platinum wires (1-mm diameter) as working electrodes, and a spiral wound 2-mm diameter carbon steel wire as a counter electrode. The carbon steel counter electrode was immersed in the salt to a depth of ~5 cm and provided a surface area that was more than 100 times larger than either the stainless steel or platinum working electrodes. The counter electrode remained in the salt throughout the series of CV runs. The stainless steel and platinum working electrodes were introduced into the salt alternately for each of the Li_2O concentrations, i.e., 0, 0.25, 0.5, 0.75, and 1.0 wt%. After each working electrode was immersed in the salt to a depth of ~1 cm, a potentiostat was used to apply a potential to the working electrode at a specified scan rate (nominally 25 mV/sec) that began at an open circuit potential and lowered (stainless steel working electrode) or rose (platinum working electrode) to a set vertex potential and then returned to the open circuit potential. The cyclic voltammagrams for the stainless steel and platinum working electrodes are shown in Figures 3 and 4.

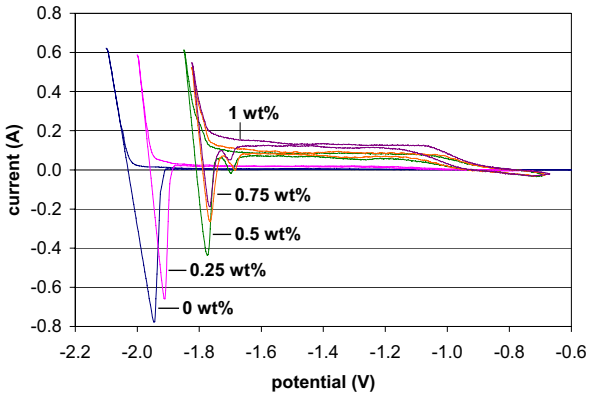

Figure 3. CV with Stainless Steel Working Electrode and Steel Counter Electrode for Varying Li_2O Concentrations

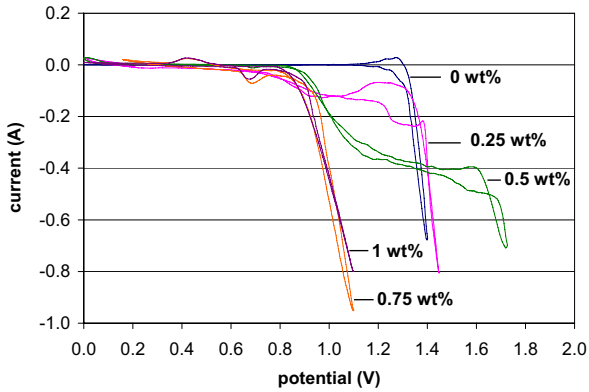

Figure 4. CV with Platinum Working Electrode and Steel Counter electrode for Varying Li_2O Concentrations

Cyclic voltammetry with the stainless steel working electrode (Figure 3) identified the cathode potential at which lithium metal was generated for the varying concentrations of lithium oxide. For the nominal lithium oxide concentration of 1 wt% in the electrolyte, the onset of lithium formation occurred at approximately -1.75 V. A notable shift in the lithium formation potential was observed between the voltammagrams for 0.25 and 0.5 wt% lithium oxide concentrations. A similar shift in reaction potential was observed with platinum as the working electrode. Specifically, the platinum dissolution potential, as shown in Figure 4, shifted from approximately +1.4 V at 0.25 wt% Li_2O to +1.65 V at 0.5 wt%. The cyclic voltammagrams at 0.75 and 1 wt% Li_2O did not reach platinum dissolution due to the current limitation (1 A) of the potentiostat. Consequently, +1.65 V was used as the upper limit for the anode potential in subsequent reduction runs to avoid platinum dissolution. The voltammagram at 1 wt% Li_2O for the platinum working electrode identified an anode potential of approximately +0.85 V at which oxygen ions began to oxidize to oxygen gas.

Cyclic voltammetry was performed on the first electrolytic reduction basket after it was loaded with spent oxide fuel and immersed in the electrolyte. The cyclic voltammagram (Figure 5) from the first reduction basket with 1 wt% Li_2O is overlain with the voltammagram for the stainless steel working electrode at 1 wt% Li_2O from Figure 3. The cyclic voltammagram for the first reduction basket clearly distinguishes the reaction zones for UO_2 reduction versus lithium reduction.

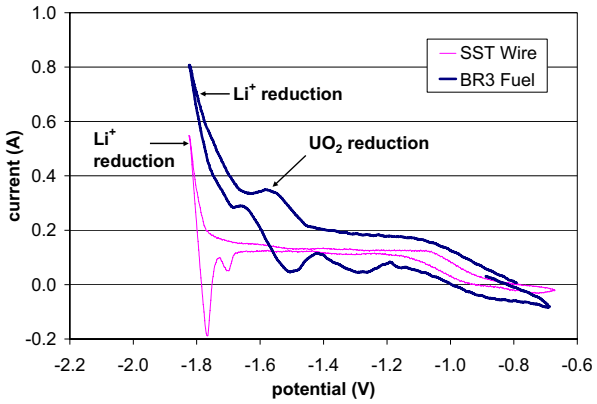

Figure 5. CV of BR3 Fuel and Stainless Steel Working Electrodes for LiCl - 1 wt% Li_2O

2. Electrolytic Reduction Operations

Following cyclic voltammetry tests, the leads from the first electrolytic reduction basket were switched from the potentiostat to the KEPCO power supplies. The platinum anode was immersed into the electrolyte, and the primary power supply was energized. The primary current (I_{Pri}) was controlled to maintain the platinum anode potential below +1.65 V. Once the potential of the basket wall approached lithium formation potential, current (I_{Sec}) was initiated from the secondary power supply. The anode (V_{Pt}), basket wall (V_{BW}), and basket center lead (V_{CL}) potentials were monitored throughout the run, as shown in Figure 6. The primary current was gradually raised to 2 A within the first 5 hours of operation, after which it was lowered to 1 A for unattended overnight operations. The primary current was raised to 2 A the next morning (after ~21 hours of run time) and then 3 A later in the day, after which both power supplies were de-energized and the platinum anode was removed for an overnight stand down. Since the anticipated end point indicators, i.e., rapidly rising anode potential or open circuit basket potential at or below lithium formation potential, were not evident, the power supplies were energized for another work shift from run time hour 30 through 37. After 36 hours of run time, the anode potential began to rise rapidly, indicating a completion of the UO_2 reduction and a consequent lowering of oxygen ion activity in the electrolyte from continued Li_2O decomposition.

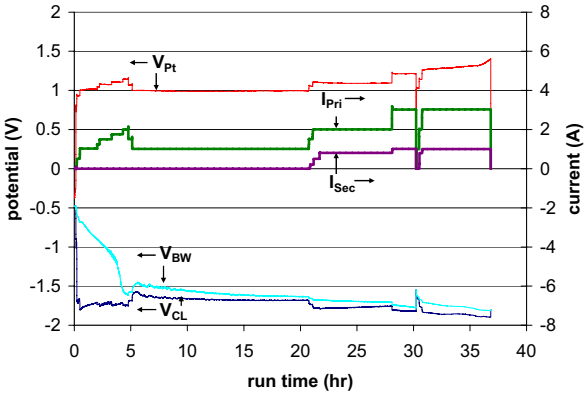

Figure 6. Response Plot from First Electrolytic Reduction Run with BR3 Spent Oxide Fuel

The cathode basket following the first electrolytic reduction run was removed and sectioned, as shown in Figure 7, revealing a metallic sheen on the cut surfaces of the packed fuel bed. The next 2 electrolytic reduction runs were conducted similarly to the first run and utilized the same molten salt electrolyte. In an effort to obtain kinetic data which necessitated a clean starting salt, the HFDA crucible was replace with a new loading of LiCl – 1 wt% Li_2O, and the fourth electrolytic reduction run was performed.

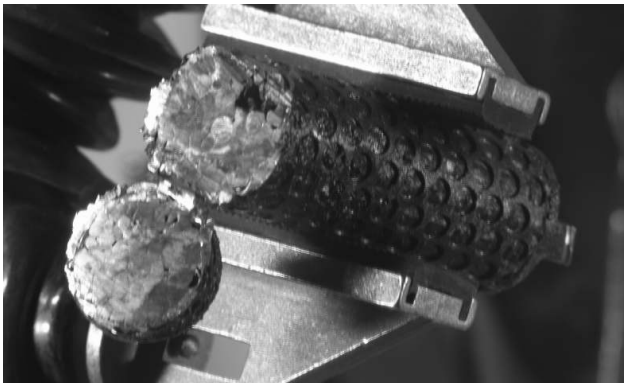

Figure 7. Post-Test Fuel Section of the First Electrolytic Reduction with BR3 Spent Oxide Fuel

Table II. Post-Test Salt and Fuel Analysis for Runs 1 - 3

Fuel Basket		*1*			*2*		*3*	
Phase	salt	*metal*	*oxide*	salt		salt		salt
units	ppm	*w%*	*w%*	ppm	*w%*	ppm	*w%*	ppm
FPS:								
Cs	ND			129 to 150		190 to 231		308 to 354
Ba	ND			85 to 140		210 to 220		310 to 330
Sr	ND			40 to 60		85 to 90		130 to 140
Rb	ND			ND		ND		ND
Te	ND			ND		ND		ND
Eu	ND			ND		ND		ND
U/TRU:								
U	6	*98*	*2*	5 to 11	*IND*	10 to 15	*IND*	3 to 9
Pu	2	*87*	*13*	0.4 to 4	"	0.6 to 0.8	"	0.4 to 1.3
Np-237	ND	*98*	*2*	ND	"	ND	"	ND
Am-241	ND	*68*	*32*	ND	"	ND	"	ND
RE:								
Nd	ND	*8*	*92*	ND	"	ND	"	ND
Ce	ND	*ND*	*>81*	ND	"	ND	"	ND
La	ND	*ND*	*>89*	ND	"	ND	"	ND
Pr	ND	*ND*	*>89*	ND	"	ND	"	ND
Sm	ND	*ND*	*>67*	ND	"	ND	"	ND
Y	ND	*ND*	*>90*	ND	"	ND	"	ND
NM:								
Zr	ND	*ND*	*ND*	ND	"	ND	"	ND
Mo	ND	*94*	*6*	ND	"	ND	"	ND
Ru	ND	*>90*	*ND*	ND	"	ND	"	ND
Tc	ND	*>94*	*ND*	ND	"	ND	"	ND
Pd	ND	*ND*	*ND*	ND	"	ND	"	ND
Rh	ND	*>75*	*ND*	ND	"	ND	"	ND

Where: RE = rare earth; U = uranium; TRU = transuranic; NM = noble metal; FPS = salt-soluble fission products; ND = non-detectable (below minimum detection levels); IND = indeterminate.

Table III. Post-Test Salt and Fuel Analysis for Run 4

Fuel Basket		*4*		
Phase	salt	*metal*	*oxide*	salt
units	ppm	*w%*	*w%*	ppm
FPS:				
Cs	ND			111 to 119
Ba	40			140
Sr	15			65
Rb	ND			ND
Te	ND			75
Eu	ND			15
U/TRU:				
U	50 to 82	*98 to 99*	*1 to 2*	2 to 5
Pu	1.9	*93 to 96*	*4 to 7*	0.3 to 0.4
Np-237	0.3	*97 to 98*	*2 to 3*	0.3 to 0.6
Am-241	ND	*77 to 84*	*16 to 23*	ND
RE:				
Nd	ND	*36 to 43*	*57 to 64*	ND
Ce	ND	*36 to 49*	*51 to 64*	ND
La	ND	*ND*	*ND*	ND
Pr	ND	*38 to 47*	*53 to 62*	ND
Sm	ND	*27 to 33*	*67 to 73*	ND
Y	ND	*34 to 40*	*60 to 66*	ND
NM:				
Zr	ND	*ND to 45*	*55 to >94*	ND
Mo	ND	*90 to 92*	*8 to 10*	ND
Ru	ND	*84 to 87*	*13 to 16*	ND
Tc	ND	*>88*	*ND*	ND
Pd	ND	*>75*	*ND*	ND
Rh	ND	*64 to 71*	*29 to 36*	ND

Where: RE = rare earth; U = uranium; TRU = transuranic; NM = noble metal; FPS = salt-soluble fission products; ND = non-detectable (below minimum detection levels).

3. Post-Test Analyses

Samples of the salt were withdrawn before and after each of the 4 electrolytic reduction runs and subjected to chemical and radiochemical analyses. The post-test salt samples for runs 1 and 2 served as pre-test salt samples for runs 2 and 3, respectively. Samples of the post-test fuel from each of the reduction runs were extracted and likewise subjected to analyses. The analytical results for the salt and fuel samples from runs 1 through 3 are shown in Table II, and those for run 4 are shown in Table III. The salt sample results identify the constituent concentrations (ppm) in the salt. The fuel sample results identify the constituents in fractions (wt%) between the metal and oxide phases. The results of the fuel samples for the second and third runs are not reported due to the questionable storage conditions of the samples (i.e., the caps to the sample containers were found to be loose after the containers had stood for a prolonged period of time in an air atmosphere prior to analysis).

Inductively Coupled Plasma – Mass Spectroscopy (ICP-MS) was used to analyze U, Pu, Np-237, and Am-241. ICP – Optical Emission Spectroscopy (ICP-OES) was used to analyze all other listed constituents except cesium, which was analyzed by atomic absorption.

IV. DISCUSSION

The distribution of fuel constituents between the salt and fuel phases behaved as expected. The salt soluble fission products cesium, barium, and strontium clearly diffused into and accumulated in the salt phase. Rubidium, tellurium, and europium were also expected to separate from the fuel and accumulate in the salt phase; however, their concentrations were largely below the detections limits for the applied ICP-OES analytical technique. Tellurium and europium, however, were detected in the salt following run 4. Even though run 4 commenced with a new salt loading and reference electrode, the same centerline thermocouple from runs 1 through 3 was used in run number 4. Consequently, some carryover of contaminated salt occurred, as evidenced by the presence of barium and strontium in the salt prior to run 4.

Since uranium and transuranic analyses in the salt phase were performed by ICP-MS, the detection limit was much lower for these constituents than the other fission products. Consequently, uranium and plutonium were detected in the salt. However, there was no clear trend in accumulation of these constituents. Also, the pre-test salt samples for runs 1 and 4 should have been devoid of fuel and yet detectable levels of uranium, plutonium and even Np-237 (in the pre-test

salt of run 4) were present. Thus, it was concluded that the minor presence of uranium and transuranic constituents in the salt phase were likely from sample contamination (due to component handling inside of a hot cell that routinely handles spent fuel), rather than from the diffusion and accumulation of BR3 fuel in the salt phase.

The reduction of metal oxides in the fuel basket occurred largely as expected, with the notable exception of zirconium. (Note: The analytical technique applied to the extent of reduction of metal oxides in the fuel basket was developmental and only validated for uranium. The technique should be applicable to the other transuranic, noble metal, and rare earth fission products. Nevertheless, without validation of each specific constituent, the results for the transuranic, noble metal, and rare earth constituents can only be considered preliminary.) The analyses of fuel from runs 1 and 4 showed a significant and comparable reduction of uranium, plutonium, and neptunium-237. The reduction of americium-241 was less significant, but still in excess of 68% for these runs. Some reduction of the rare earths was observed, notably in run 4, where roughly one third of the rare earth constituents were found in the metal phase. The noble metal constituents were predominantly found in the metal phase for fuel from runs 1 and 4 with the exception of zirconium. Zirconium was not identified in either the metal or oxide phases of the fuel from run 1. Suspecting that the zirconium remained in the oxide phase, an additional step was applied to the analysis of fuel from run 4 which involved dissolution of the oxide phase with hydrofluoric acid to adequately dissolve any zirconium in the oxide phase. Zirconium was consequently detected in the metal phase for fuel from run 4. However, the zirconium was predominantly observed in the oxide phase (i.e., 55 to 94 wt%).

Another observation that is noteworthy is the cell efficiency. Both runs 1 and 4 exhibited a nearly identical cell efficiency of approximately 38%. These cell efficiencies were calculated from the ratio of theoretical charge for the given fuel loading to the actual applied charge from primary current during manned operations. These reported cell efficiencies are approximate values since they include some reduction of lithium oxide in addition to uranium oxide. A true measure of uranium oxide reduction completion alone would have resulted in a cell efficiency that was considerably higher than 38%.

V. CONCLUSIONS

The electrolytic reduction of spent light water reactor oxide fuel was successfully demonstrated at bench-scale in a hot cell at the INL Materials and Fuels Complex. Objectives of the tests were met. The extent of reduction of metal oxides was determined which was in excess of 98% for uranium. The distribution of fission products between the salt and fuel phases was also quantified. Cesium, barium, and strontium diffused from the fuel and accumulated in the salt phase, as expected. The rare earth and noble metal fission products remained with the uranium and transuranic constituents in the reduced fuel basket. The rare earth and zirconium fission products remained predominantly as oxides in the reduced fuel basket. The impact of fission product accumulation on the electrolytic reduction process was inconclusive, due to an insufficient build-up of fission products in the electrolyte. The impact of fission product accumulation on the electrolytic reduction process is subject to further examination.

ACKNOWLEDGMENTS

This work was supported under U.S. Department of Energy contract W-31-109-ENG-38.

REFERENCES

1. R. W. Benedict and H. F. McFarlane, “EBR-II Spent Fuel Treatment Demonstration Project Status,” *RADWASTE*, Vol. 5, Issue 4 (1998).

2. K. Gourishankar, L. Redey, and M. Williamson, “Electrolytic Reduction of Metal Oxides in Molten Salts,” *Light Metals*, ed., W. A. Schneider, Warrendale, PA, The Minerals, Metals, and Materials Society (2002).

3. S. D. Herrmann, S. X. Li, M. F. Simpson, D. R. Wahlquist, “Electrolytic Reduction of Spent Oxide Fuel – Bench-Scale Test Preparations,” Proc. ANS Fifth Topical Meeting on DOE Spent Nuclear Fuel and Fissile Materials Management, Charleston, SC, September (2002).

4. *HSC Chemistry – Chemical Reaction and Equilibrium Software with Extensive Thermochemical Database*, Version 5.1, Outokumpu Research Oy, Finland, (2002).